

## 3- $\mu\text{m}$ mid-infrared polarization-independent and CMOS-compatible graphene modulator

LU Rong-Guo<sup>1\*</sup>, LIN Rui<sup>1</sup>, SHEN Li-Ming<sup>1</sup>, CAI Song-Wei<sup>1</sup>, WANG Yu-Jiao<sup>1</sup>, CHEN Jin-Zhan<sup>1</sup>,  
YANG Zhong-Hua<sup>2</sup>, LYU Jiang-Bo<sup>1</sup>, ZHOU Yong<sup>1</sup>, WANG Xiao-Ju<sup>1</sup>, LIU Yong<sup>1</sup>

- (1. State Key Laboratory of Electronic Thin Films and Integrated Devices, School of Optoelectronic Science and Engineering, University of Electronic Science and Technology of China, Chengdu 610054, China;  
2. Chongqing United Microelectronics Center, Chongqing 401332, China)

**Abstract:** This paper proposes a 3- $\mu\text{m}$  mid-infrared band polarization-independent and CMOS-compatible graphene modulator, which mainly includes two parts: the mode conversion structure and the graphene modulator. This modulator not only fulfills the requirement of compatibility with CMOS, but also can achieve polarization-independent modulation of the fundamental mode. Simulation results show that this modulator can achieve an extinction ratio (ER) higher than 20 dB in the mid-infrared band from 2.95  $\mu\text{m}$  to 3.05  $\mu\text{m}$ , the insert loss for both TE and TM modes are less than 1.3 dB, and polarization-dependent loss is less than 1.09 dB. Through the calculation, the 3 dB bandwidth up to 9.47 GHz can be obtained when the length of the device is 420  $\mu\text{m}$ .

**Key words:** graphene modulator, polarization-independent, mode conversion, mid-infrared

## 3- $\mu\text{m}$ 中红外偏振无关且 CMOS 兼容的石墨烯调制器

陆荣国<sup>1\*</sup>, 林 瑞<sup>1</sup>, 沈黎明<sup>1</sup>, 蔡松炜<sup>1</sup>, 王玉姣<sup>1</sup>, 陈进湛<sup>1</sup>, 杨忠华<sup>2</sup>, 吕江泊<sup>1</sup>,  
周 勇<sup>1</sup>, 王小菊<sup>1</sup>, 刘 永<sup>1</sup>

- (1. 电子薄膜与集成器件国家重点实验室, 光电科学与工程学院, 电子科技大学, 四川 成都 610054;  
2. 重庆微电子中心, 重庆 401332)

**摘要:** 文章提出了一种 3- $\mu\text{m}$  中红外波段偏振无关且 CMOS 兼容的石墨烯调制器, 器件主要包括两部分: 模式转换结构及石墨烯调制器。该调制器不仅满足 CMOS 兼容的要求, 而且能够实现基膜的偏振无关调制。仿真结果表明该调制器在 2.95  $\mu\text{m}$  到 3.05  $\mu\text{m}$  的中红外波段能够实现高于 20 dB 的消光比, TE 和 TM 模式的插入损耗都低于 1.3 dB, 其偏振相关损耗低于 1.09 dB。通过计算, 当器件长度为 420  $\mu\text{m}$ , 能够获得高达 9.47 GHz 的 3 dB 带宽。

**关键词:** 石墨烯调制器; 偏振无关; 模式转换; 中红外  
**中图分类号:** O43

**文献标识码:** A

### Introduction

A variety of functional electro-optic materials, such as graphene<sup>[1]</sup>, chalcogenide<sup>[2]</sup>, and black phosphorus<sup>[3]</sup>, have been discovered in recent years, which indi-

rectly promoted the realization of high-performance electro-optic devices. Among these materials, graphene has been widely used in many fields with its unique physics properties<sup>[4-8]</sup>, especially in electro-optic modulators. Compared with other materials, the advantage of gra-

**Received date:** 2020-09-04, **revised date:** 2021-02-27

**收稿日期:** 2020-09-04, **修回日期:** 2021-02-27

**Foundation items:** Supported by the National Key Research and Development Program of China (2018YFE0201901); the Program for International S&T Cooperation Projects of Sichuan Province (2020YFH0108); the National Nature Science Foundation of China (61435010, 61307070, 61421002, 61704021); the Fundamental Research Funds for the Central Universities (ZYGX2019J046).

**Biography:** Lu Rong-Guo (1982-), male, Guangxi, PhD. Research area involves Integrated optics, Optical communication, and Microwave photonics. E-mail: lurongguo@uestc.edu.cn.

\* **Corresponding author:** E-mail: lurongguo@uestc.edu.cn

phene includes constant absorption over a wide spectrum<sup>[9]</sup>, ultra-high carrier mobility under room temperature<sup>[10]</sup>, controllable conductivity, and compatibility with CMOS. The light in the mid-infrared band has attracted wide attention in the fields of communications, homeland security, and biomedicine. Some electro-optic modulators operating in the mid-infrared band have been reported, but most of them are polarization-dependent<sup>[11-14]</sup>, which means that the device can operate under only one polarization state.

Research work has proven that the graphene is an anisotropic material<sup>[15-16]</sup> whose lattice is only periodically arranged along the 2D surface of graphene. Graphene mainly interacts with the tangential electric field of electromagnetic waves<sup>[12]</sup>, and this characteristic will lead to the interaction between the graphene horizontally embedded in the waveguide and the TM mode is much stronger, which has been confirmed in previous work<sup>[17]</sup>. In the previously reported graphene-based polarization-independent modulators<sup>[18-21]</sup>, most of them need to face the problem of the complicated structure of the device, cumbersome manufacturing processes, and incompatibility with CMOS. Therefore, achieving the polarization-independent operation of the electro-optic modulator remains a challenge.

In this paper, we propose a 3- $\mu\text{m}$  mid-infrared polarization-independent and CMOS-compatible graphene modulator. The  $\text{TE}_0$  mode of incident light is converted to the  $\text{TM}_0$  mode through a mode conversion structure, and the  $\text{TM}_0$  mode of incident light is not affected by this structure because of the phase mismatching, so we can achieve the modulation of only  $\text{TM}_0$  mode through the graphene modulator. In the structure of the graphene modulator, the graphene sheet is integrated on the chalcogenide glass to fulfill the compatibility with CMOS. Simulation results show that this modulator can achieve the polarization-independent operation in the mid-infrared band. The length of the device is designed to be 420

$\mu\text{m}$ , we can obtain the ER higher than 20 dB, and the insert loss less than 1.3 dB. The polarization-dependent loss is maintained at a value less than 1.09 dB in the wavelength range from 2.95  $\mu\text{m}$  to 3.05  $\mu\text{m}$ , and the 3 dB bandwidth of the device is 9.47 GHz through the calculation.

## 1 Principle and structure design

The structure of our proposed device is shown in Fig. 1 (a). The device mainly includes two parts, the mode conversion structure and the graphene modulator. Since the graphene horizontally integrated on the chalcogenide glass mainly interacts with  $\text{TM}_0$  mode, we designed a mode conversion structure composed of the asymmetric directional coupler (ADC) and adiabatic taper (AT). As shown in Fig. 1 (b), we designed two modulation waveguide arms in the device, the width of arm2 is 1.5  $\mu\text{m}$ , and compared with arm 2, arm 1 adds a wide waveguide with the size of 3.1  $\mu\text{m}$  and a tapered waveguide, the spacing between the two arms is set to 1  $\mu\text{m}$  to prevent mode coupling. The  $\text{TE}_0$  mode is converted to  $\text{TE}_1$  mode by the ADC composed of a narrower waveguide and a wider waveguide, then the  $\text{TE}_1$  mode is converted to the  $\text{TM}_0$  mode by the AT, so we can realize the modulation of  $\text{TM}_0$  mode in the modulation area. At the output of arm1, the  $\text{TM}_0$  mode will be restored to the  $\text{TE}_0$  mode by the same mode conversion structure. In the meanwhile, the  $\text{TM}_0$  mode will not be affected when passing through the region of ADC because of phase mismatching. By using this principle, the device we proposed can achieve the same modulation capability for both TE and TM mode.

In order to achieve polarization-independent modulation, we horizontally integrated the graphene sheet on the chalcogenide glass. When a certain voltage is applied to graphene, its chemical potential will be dynamically changed. Graphene is an anisotropic material, its

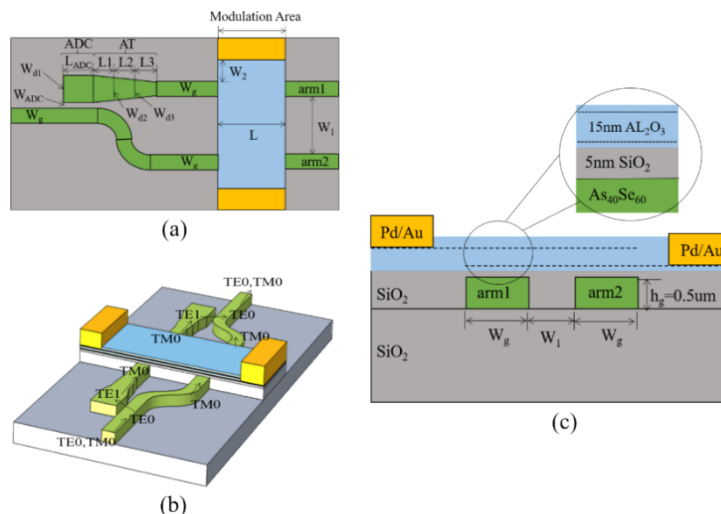


Fig. 1 (a) Schematic diagram of our proposed device, (b) schematic diagram of mode conversion structure, (c) cross-sectional schematic diagram of the graphene modulator

图1 (a) 器件的结构示意图, (b) 模式转化结构示意图, (c) 石墨烯调制器的横截面示意图

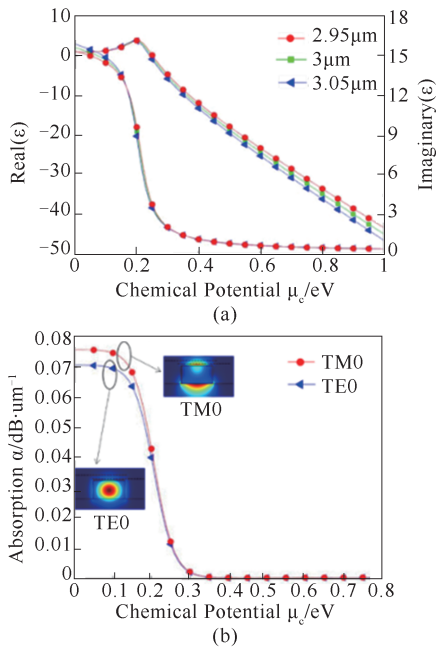


Fig. 2 (a) Under the wavelength of 2.95  $\mu\text{m}$ , 3  $\mu\text{m}$ , 3.05  $\mu\text{m}$ , the in-plane dielectric constant changes with the applied voltage, (b) the variation of the absorption coefficient for both TE<sub>0</sub> and TM<sub>0</sub> mode of graphene modulator under different chemical potential

图2 (a) 波长为 2.95  $\mu\text{m}$ , 3  $\mu\text{m}$ , 3.05  $\mu\text{m}$  时面内介电常数随施加电压的变化, (b) 不同石墨烯化学势下石墨烯调制器对 TE<sub>0</sub> 和 TM<sub>0</sub> 模式吸收的变化情况

vertical dielectric constant is not affected by the applied voltage and is always maintained at a value of 2.5, while the in-plane dielectric constant is determined by<sup>[10]</sup>

$$\epsilon = 1 + \frac{i\delta}{\omega\epsilon_0 t_g} \quad (1)$$

It can be seen from the formula that the in-plane dielectric constant mainly depends on the frequency of incident light and applied voltage. As shown in Fig. 2(a), under the wavelength of 2.95  $\mu\text{m}$ , 3  $\mu\text{m}$ , 3.05  $\mu\text{m}$ , the variation of the in-plane dielectric constant under different graphene chemical potential is analyzed. The absorption characteristic of graphene mainly depends on its dielectric constant, Fig. 2(b) shows the variation of the absorption coefficient for both TE<sub>0</sub> and TM<sub>0</sub> mode under different graphene chemical potential. It can be seen that the absorption coefficient for both TE<sub>0</sub> and TM<sub>0</sub> modes decrease rapidly when the graphene chemical potential increases. In addition, the absorption coefficient for the TM<sub>0</sub> mode is greater than the TE<sub>0</sub> mode, which means that the graphene sheet has a stronger interaction with TM<sub>0</sub> mode.

The cross-section of the graphene modulator is shown in Fig. 1(c). By using an electron beam exposure method<sup>[22]</sup>, a 0.5- $\mu\text{m}$  thick chalcogenide glass waveguide is integrated on the silicon-based platform, then a 5 nm thick SiO<sub>2</sub> isolation layer is thermally grown on the surface of the waveguide. Afterward, two-layer CVD-grown graphene sheets were transferred on top of the chalcogenide glass waveguide<sup>[23]</sup>. By using the thermal atom

deposition method<sup>[24]</sup>, two-layer graphene sheets were separated with a 15 nm thick Al<sub>2</sub>O<sub>3</sub> to form a capacitor structure. In the meanwhile, in order to prevent the latent carrier injection, the upper and lower layer of graphene sheets were separated from the chalcogenide waveguide and the air with a 5 nm thick Al<sub>2</sub>O<sub>3</sub> isolation layer. Finally, the metal electrode Au/Pd is transferred onto the graphene sheet, in order to avoid interference with the optical mode in the waveguide, the electrode is located 0.6  $\mu\text{m}$  away from the waveguide.

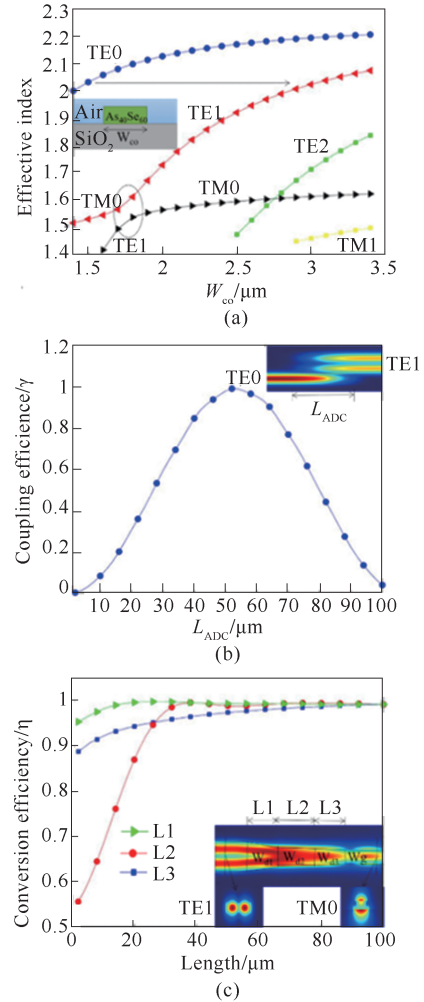


Fig. 3 (a) The variation of effective refractive index for the first five modes in the width range from 1.4  $\mu\text{m}$  to 3.4  $\mu\text{m}$ , (b) analyzing the influence on coupling efficiency by sweeping the coupling length, (c) analyzing the influence on conversion efficiency by sweeping the length of three parts

图3 (a) 前5个模式的有效折射率在 1.4  $\mu\text{m}$  到 3.4  $\mu\text{m}$  的波导宽度下的变化情况, (b) 通过扫描耦合长度, 分析其对耦合效率的影响, (c) 扫描 AT 结构三部分的长度, 分析其对转换效率的影响

The performance of the device is simulated by using Lumerical software. The variation of the effective mode index under different width of waveguide is analyzed, as shown in Fig. 3(a), the waveguide structure is composed of SiO<sub>2</sub> as the lower cladding, air as the upper cladding,

and chalcogenide glass as the core. We analyzed the effective refractive index of the first five modes in the width range from 1.4  $\mu\text{m}$  to 3.4  $\mu\text{m}$ . It can be seen that the effective refractive index of  $\text{TE}_0$  mode in a width of 1.5  $\mu\text{m}$  is close to the value of  $\text{TE}_1$  mode in a width of 3.1  $\mu\text{m}$ , so we choose an ADC composed of these two sizes of the waveguide to achieve the conversion from  $\text{TE}_0$  to  $\text{TE}_1$  mode, and the coupling spacing is set at 0.1  $\mu\text{m}$ . As shown in Figure 3(b), when the coupling length is 50  $\mu\text{m}$ , the coupling efficiency up to 0.97 can be obtained, and the electric field distribution of mode coupling is shown in the inset of Figure 3(b). In addition, when the width of the waveguide is around 1.75  $\mu\text{m}$ , the  $\text{TE}_1$  and the  $\text{TM}_0$  mode are both in the mode mixing region, so we can design a tapered waveguide with the size around 1.75  $\mu\text{m}$  to realize the conversion from  $\text{TE}_1$  mode to  $\text{TM}_0$  mode. The width of input and output of taper is 3.1  $\mu\text{m}$  and 1.5  $\mu\text{m}$ , in order to achieve mode conversion, we divided the taper into three parts, the width of the input and output of the second part is set at 1.81  $\mu\text{m}$  and 1.67  $\mu\text{m}$ . As shown in Fig. 3(c), the influence of the length for three parts on conversion efficiency is analyzed by the simulation, the main impact on conversion efficiency are the second part, so we choose  $L_1 = L_2 = L_3 = 20 \mu\text{m}$  to maximize the conversion efficiency and reduce the size of the device as much as possible. The electric field distribution of mode conversion is shown in the inset of Fig. 3(c).

## 2 Modulator Performance

We analyzed the insert loss of the device, including the mode coupling loss of the ADC(CL1), the mode conversion loss of the AT(CL2), the insert loss between the waveguide arm and the graphene modulator(IL), and the graphene absorption loss (GL). Figure 2(b) shows the variation of the absorption coefficient of the fundamental mode under different graphene chemical potential, it can be seen that when the applied voltage is 0.1 eV and 0.7 eV, the absorption coefficient reaches a maximum and minimum respectively. Therefore, we choose 0.1 eV and 0.7 eV as the "OFF" state point and the "ON" state point respectively. In order to obtain a higher ER, the length of the graphene modulator is set to 300  $\mu\text{m}$ . As shown in Fig. 4(a), the variation on insert loss for different parts is analyzed under the wavelength range from 2.95  $\mu\text{m}$  to 3.05  $\mu\text{m}$ . The normalized transmission and extinction ratio of our proposed device are also analyzed, as shown in Fig. 4(b). The propagation loss under the "ON" state point is mainly determined by the absorption loss of graphene and its value is less than 1.3 dB, while under the "OFF" state point, the normalized transmission is less than -20 dB and the extinction ratio is higher than 20 dB. In order to measure the polarization-dependent loss, we analyzed the normalized transmission difference between the two modes, the results show that the polarization-dependent loss of the device is less than 1.09 dB in the wavelength range from 2.95  $\mu\text{m}$  to 3  $\mu\text{m}$ , which fulfills the requirement of polarization-independent

modulation.

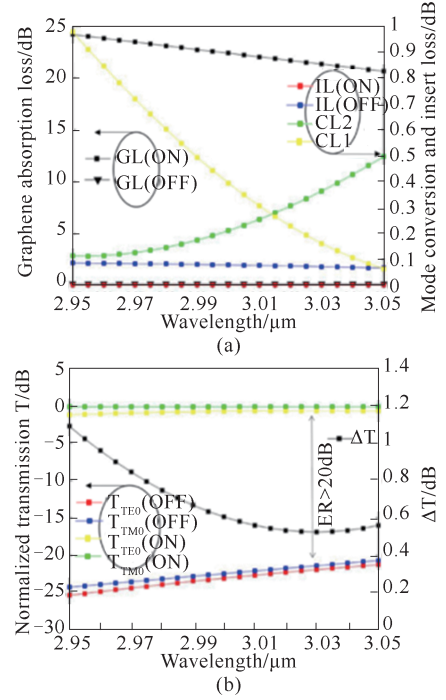


Fig. 4 (a) The variation of insertion loss of various parts for the device under the wavelength from 2.95  $\mu\text{m}$  to 3.05  $\mu\text{m}$ , (b) the normalized transmission of the device under the wavelength from 2.95  $\mu\text{m}$  to 3.05  $\mu\text{m}$

图4 (a) 波长从 2.95  $\mu\text{m}$  变化到 3.05  $\mu\text{m}$ , 器件各部分插入损耗的变化, (b) 器件在 2.95  $\mu\text{m}$  到 3.05  $\mu\text{m}$  波长范围内的归一化透射率

The 3 dB modulation bandwidth  $f_{3dB}$  is also a crucial parameter for the modulator. Due to the ultra-high carrier mobility of graphene under room temperature, the operating speed of the modulator is no longer limited by the lifetime of minority carriers. The main factor affecting 3 dB modulation bandwidth of modulator based on graphene is RC delay. The result is expressed as

$$f_{3dB} = \frac{1}{2\pi RC} \quad (2)$$

$R$  is the entire resistance of the device, mainly including two parts, the contact resistance  $R_c$  between graphene sheets and electrodes, and the graphene sheets resistance  $R_s$ , which can be calculated by

$$R = \frac{2R_c}{L} + \frac{2R_s(2w_g + w_1 + w_2)}{L} \quad (3)$$

where  $w_g$  is the effective width of graphene,  $w_1$  is the spacing between two modulation arms,  $w_2$  is the width of graphene from metal contact to the active region of the waveguide,  $L$  is the length of graphene,  $R_s = 200 \Omega / \text{sq}^{-1}$ [25] and  $R_c = 100 \Omega \cdot \mu\text{m}$ [26] can be obtained from previous work.

$C$  is the capacitance of the capacitor composed of two graphene sheets. To estimate the 3 dB bandwidth, we regarded the capacitor structure of the device as a parallel plate capacitor. The estimated 3 dB bandwidth is

9.47 GHz, in addition, the RC delay problem may be solved in the future, which means that a higher 3dB bandwidth can be obtained<sup>[27-28]</sup>.

### 3 Conclusion

This paper proposes a 3- $\mu\text{m}$  mid-infrared polarization-independent and CMOS-compatible graphene modulator. In the structure of this device, in order to achieve polarization-independent modulation, we introduce an asymmetric directional coupler and adiabatic taper structure to achieve mode conversion, and the graphene sheet is integrated on the chalcogenide glass waveguide. The simulation results show that our device can achieve an extinction ratio higher than 20 dB under the mid-infrared band from 2.95  $\mu\text{m}$  to 3.05  $\mu\text{m}$ , the insert loss for both two modes is less than 1.3 dB, and the polarization-dependent loss is less than 1.09 dB. These data indicate that our device fully fulfills the requirement of the polarization-independent operation. Through the calculation, when the length of the device is 420  $\mu\text{m}$ , the 3 dB bandwidth up to 9.47 GHz can be obtained, and after solving the RC delay problem in the future, it is expected to achieve a higher 3 dB bandwidth. In short, this new type of 3  $\mu\text{m}$  mid-infrared polarization-independent and CMOS-compatible modulator is expected to promote the development of on-chip optical communications in the future.

### References

- [1] Novoselov K S, Geim A K, Morozov S V, *et al.* Electric field effect in atomically thin carbon films [J]. *Science (New York, N. Y.)*, 2004, **306**(5696): 666-669.
- [2] K. F. Mak, C. Lee, J. Hone, *et al.* Atomically thin MoS<sub>2</sub>: A new direct-gap semiconductor [J]. *Phys. Rev. Lett.*, 2010, **105** (13): 136805.
- [3] L. Li *et al.* Black phosphorus field-effect transistors [J]. *Nature Nanotechnol.*, 2014, **9**(5): 372-377.
- [4] K. S. Novoselov, A. K. Geim, S. V. Morozov, *et al.* Two-dimensional gas of massless Dirac fermions in graphene [J]. *Nature*, 2005, **438** (7065): 197.
- [5] N. Song, H. Q. Fan, H. L. Tian. Reduced graphene oxide/ZnO nanohybrids: Metallic Zn powder induced one-step synthesis for enhanced photocurrent and photocatalytic response [J]. *Applied Surface Science*, 2015, **353**: 580-587.
- [6] H. L. Tian, H. Q. Fan, J. W. Ma, *et al.* Noble metal-free modified electrode of exfoliated graphitic carbon nitride/ZnO nanosheets for highly efficient hydrogen peroxide sensing [J]. *Electrochimica Acta*, 2017, **247**: 787-794.
- [7] J. W. Fang, H. Q. Fan, M. M. Li, *et al.* Nitrogen self-doped graphitic carbon nitride as efficient visible light photocatalyst for hydrogen evolution [J]. *Journal of Material Chemistry A*, 2015, **3** (26): 13819-13826.
- [8] T. J. Echtermeyer, L. Britnell, P. K. Jasnós, *et al.* Strong plasmonic enhancement of photovoltage in graphene [J]. *Nature Communications*, 2011, **2**(1): 458.
- [9] R.R Nair, P. Blake, A.N. Grigorenko, K.S. *et al.* Fine structure constant defines visual transparency of graphene [J]. *Science*, 2008, **320** (5881): 1308.
- [10] K.I. Bolotin, K. Sikes, Z. Jiang, *et al.* Stormer. Ultrahigh electron mobility in suspended graphene [J]. *Solid State Commun.* 2008, **146** (9-10): 351-355.
- [11] M. Sadeghi, B. Janjan, Heidari, D. Abbott. Mid-infrared hybrid Si/VO<sub>2</sub> modulator electrically driven by graphene electrodes [J]. *Optics Express*, 2020, **28**(7): 9198-9207.
- [12] J. Chi, H.J. Liu, N. Huang, *et al.* A broadband enhanced plasmonic modulator based on double-layer graphene at mid-infrared wavelength [J]. *Journal of Physics D-Applied Physics*, 2019, **52** (44): 445101.
- [13] M. Cai, S.L. Wang, B. Gao, *et al.* A New Electro-Optical Switch Modulator Based on the Surface Plasmon Polaritons of Graphene in Mid-Infrared Band [J]. *Sensors*, 2019, **19**(1): 89.
- [14] Yamaguchi Y, Takagi S, Takenaka M. Low-loss graphene-based optical phase modulator operating at mid-infrared wavelength [J]. *Jpn. J. Appl. Phys.* 2018, **57**: 401 - 406.
- [15] R. Hao, W. Du, E. P. Li, *et al.* Graphene assisted TE/TM independent polarizer based on Mach-Zehnder interferometer [J]. *IEEE Photon. Technol. Lett.*, 2015, **27**(10): 1112-1115.
- [16] Z. S. Chang, K. S. Chiang. Experimental verification of optical models of graphene with multimode slab waveguides [J]. *Optics Letter*, 2016, **41**(9): 2129-2132.
- [17] S. J. Koester, M. Li. High-speed waveguide-coupled graphene-on-graphene optical modulators [J]. *Appl. Phys. Lett.*, 2012, **100** (21): 171107.
- [18] S.W. Ye, D. Liang, R.G. Lu, *et al.* Polarization-independent modulator by partly tilted graphene-induced electro-absorption effect [J]. *IEEE Photonics Technology Letters*, 2017, **29** (1): 23-26.
- [19] XIAO H, GUI C, JIAN W. A Graphene-based Polarization-Insensitive Optical Modulator [C]// Integrated Photonics Research, Silicon & Nanophotonics. 2014.
- [20] X. Peng, E. Li, R. Hao. Graphene-aluminum oxide meta material for a compact polarization-independent modulator [C]. Advanced Materials and Processes for RF and THz Applications (IMWS-AMP), 2015 IEEE MTT-S International Microwave Workshop Series on, IEEE, 2015, 1 - 3.
- [21] M. K. Shah, R. Lu, D. Peng, *et al.* Graphene-assisted polarization-insensitive electro-absorption optical modulator [J]. *IEEE Transactions on Nanotechnology*, 2017, **16**(6): 1004 - 1010.
- [22] A Di Falco, M Massari, M G Scullion, *et al.* Propagation losses of slotted photonics crystal waveguide [J]. *IEEE Photon Journal*, 2012, **4**(5): 1536-1541.
- [23] X. Li, W. Cai, J. An, *et al.* Large-area synthesis of high-quality and uniform graphene films on copper foils [J]. *Science*, 2009, **324** (5932): 1312 - 1314.
- [24] C. T. Phare, Y.-H. D. Lee, J. Cardenas, *et al.* Graphene electro-optic modulator with 30 Ghz bandwidth [J]. *Nature Photonics*, 2015, **9** (8): 511.
- [25] W. W. Cai, Y. W. Zhu, X. S. Li, *et al.* Large area few-layer graphene/graphite films as transparent thin conducting electrodes [J]. *Appl. Phys. Lett.*, 2009, **95**(12): 123115.
- [26] ZHONG H, ZHANG Z, CHEN B, *et al.* Realization of low contact resistance close to theoretical limit in graphene transistors [J]. *Nano Research*, 2015.
- [27] S. de, N. J. Coleman. Are there fundamental limitations on the sheet resistance and transmittance of thin graphene films? [J]. *ACS Nano*, 2010, **4**(5): 2713-2720.
- [28] W. Li, Y. Liang, D. Yu, *et al.* Ultraviolet/ozone treatment to reduce metal-graphene contact resistance [J]. *Appl. Phys. Lett.* 2013, **102** (18): 183110.